TRANSACTIONS OF THE INSTITUTE OF FLUID-FLOW MACHINERY

No. 136, 2017, 55–64

Miachał Stajnke[1]* and Wojciech Włodarski[2]

How much a geometrical model of a honeycomb seal can be simplified in the CFD calculation

[1] *Department of Energy Conversion, Institute of Fluid Flow Machinery, Polish Academy of Sciences, Fiszera 14, 80-231 Gdańsk, Poland*

[2] *Faculty of Mechanical Engineering, Gdansk University of Technology, Siedlicka 4, 80-001 Gdańsk, Poland*

Abstract

This paper presents the influence of geometry simplification on the results obtained in the computational fluid dynamics simulation. The subject of simulation was part of the honeycomb seal located at the inlet to high pressure part of a steam turbine. There were three different geometrical models assumed in the calculations. First one was two-dimensional case and two others were three-dimensional, one with the radius of curvature and one without. Numerical simulations were performed for 15 sets of boundary conditions to compare flow characteristics for each geometrical case.

Keywords: CFD modeling; Steam turbine; Seal; Honeycomb

1 Introduction

There is natural need for improvement in every human. This desire can be seen in the everyday aspects of our lives as we try to make things better and faster. Power engineering is no different on that field. Constructors from all around the world have to deal with the problem of constantly rising energy consumption. Because of that, even the smallest profit in terms of efficiency in the process of energy conversion is quite important. When it comes to steam turbines, which

*Corresponding author. E-mail address: mstajnke@imp.gda.pl

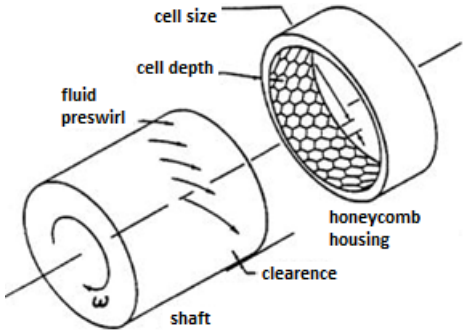

Figure 1. Structure and idea of the honeycomb seal [16].

are the biggest and most popular energy producing devices, the internal seals are very relevant for obtaining highest possible performance [7,12,13,20].

From the variation of the seal types, the honeycomb structure of the seal gains more and more interests since the 80's [15,16]. The visualisation of the seal can be seen in Fig. 1 [16]. Due to high resilience of the honeycomb seal it quickly become very popular and has been widely studied [2,4,6]. First research approach is usually empirical. Some early works concerning honeycomb seal seems to confirm this trend [3,10]. With technological progress, experiments are no longer the only source of knowledge of phenomena that occur inside the seals. In that field computational fluid dynamics (CFD) has started building its position and is widely used in analysing power machinery [12,14,19,20].

2 Model adopted to CFD calculations

Constantly rising computing power of supercomputers as well as small personal computers allows to perform quick numerical simulations with high accuracy. In this paper numerical calculations were performed in popular CFD software Ansys Fluent, which serves as solver to the Navier-Stokes equations using finite volume method.

There are extensive science works dealing with problems of vortex flows and turbulence modeling. Basis of these problems are widely described in many standard literature items [1,9,18]. Turbulent flows are characterized by a variable velocity field. The transition from laminar to turbulent flow occurs when Reynolds number, which through is one of the criteria to determine the type of the flow, exceeds a critical value under the dependence of the geometry which the fluid flows. Nonlinear form of the Navier-Stokes equations, describing the fluid flow, causes an increase of disruption in the stream when the Reynolds number exceeds a critical value. This instability leads to changes in velocity field, pressure and

temperature.

One of the ways to deal with the problem of simulation of turbulent flows are Reynolds-averaged Navier-Stokes (RANS) equations, which separate the components of the velocity field into the mean (time-averaged) component and fluctuating component. Direct numerical simulations (DNS), in which all time and length scales were solved, are too expensive to use them in practical problems with available computing resources. The RANS equation (when mean flow is stable) in the Cartesian coordinate system is represented by formula

$$\overline{U}_k \frac{\partial \overline{\rho U_i}}{\partial \chi_k} = -\frac{\partial \overline{P}}{\partial \chi_i} + \mu \frac{\partial^2 \overline{U_i}}{\partial \chi_k \partial \chi_k} - \frac{\partial \overline{\left(\partial u_i' u_k'\right)}}{\partial \chi_k}\,, \qquad i,k = 1,2,3\,, \tag{1}$$

where:

$\overline{U}_k$ –average velocity vector,

$\frac{\partial \overline{\rho U_i}}{\partial \chi_k}$ –derivative by χ variable of average speed tensor,

$\frac{\partial \overline{P}}{\partial \chi_i}$ –average pressure partial derivative,

μ –viscosity,

$\frac{\partial^2 \overline{U_i}}{\partial \chi_k \partial \chi_k}$ –second derivative with respect of verage speed tensor,

$\frac{\partial \overline{\left(\partial u_i' u_k'\right)}}{\partial \chi_k}$ –derivative with respect to x of Reynolds stress tensor.

The equations describing average flow of fluid will be solvable only if we could model the influence of the flow fluctuation on the average flow. Reynolds stress tensor in the above equation is represented by element $\partial \overline{u_i' u_k'}$. This element appears in RANS equation due to flow fluctuations and thermal convection. Averaged turbulent flow behaves similar to laminar flow with different fluid viscosities between layers. Therefore, Reynolds stress tensor can be modeled by turbulent viscosity, μ_t, what is explained by the following equation:

$$\overline{U}_k \frac{\partial \overline{\rho U_i}}{\partial \chi_k} = -\frac{\partial \overline{P}}{\partial \chi_i} + (\mu + \mu_t) \frac{\partial^2 \overline{U_i}}{\partial \chi_k \partial \chi_k}\,. \tag{2}$$

The k-ε model, used in the presented work, consists the set of two equations in which turbulent viscosity is expressed by energy of kinetic turbulence, k, and energy dissipation, ε:

$$\mu_t = \rho C_\mu \frac{k^2}{\varepsilon}\,, \tag{3}$$

where C_μ is constant and equals 0.09.

If kinetic energy and dissipation are constant, component associated with fluctuations in velocity is defined as

$$k = \frac{1}{2}\overline{u_i' u_i'}\,, \tag{4}$$

$$\varepsilon = \frac{\mu}{\rho}\overline{\left(\frac{\partial u_i'}{\partial \chi_k}\frac{\partial u_i'}{\partial \chi_k}\right)}\,. \tag{5}$$

Since the equations precisely defining k and ε are not known, the standard k-ε model uses the following transport equations:

$$\frac{\partial(\rho k)}{\partial t} + \frac{\partial(\rho k u_j)}{\partial \chi_j} = \frac{\partial}{\partial \chi_j}\left[\left(\mu + \frac{\mu_t}{\sigma_k}\right)\frac{\partial k}{\partial \chi_j}\right] + G_k + G_b - \rho\epsilon - Y_M + S_k\,, \tag{6}$$

$$\frac{\partial(\epsilon\varepsilon)}{\partial t} + \frac{\partial(\rho\varepsilon u_j)}{\partial \chi_j} = \frac{\partial}{\partial \chi_j}\left[\left(\mu + \frac{\mu_t}{\sigma_\varepsilon}\right)\frac{\partial \varepsilon}{\partial \chi_j}\right] + C_{1\varepsilon}(G_k + C_{3\varepsilon}G_b) - C_{2\epsilon}\rho\frac{\varepsilon^2}{k} + S_\varepsilon\,, \tag{7}$$

where:

G_k	–	velocity gradient forming part of the kinetic energy of turbulence defined as $2\mu_t\frac{\partial\overline{U_i}}{\partial\chi_j}\frac{\partial\overline{U_i}}{\partial\chi_j}$,
G_b	–	buoyant force, usually neglected in gas flows,
Y_M	–	fluctuations resulting from changes in turbulence,
S_k, S_ε	–	the initial conditions,
σ_k σ_ε	–	experimentally designated turbulence Prandtl numbers for the kinetic energy of turbulence, equal to 1.0 and 1.3, respectively,
$C_{1\varepsilon}$, $C_{2\varepsilon}$, $C_{3\varepsilon}$	–	constants experimentally determined for k-ε model, equal to: $C_{1\varepsilon} = 1.44$, $C_{2\varepsilon} = 1.92$ and $C_{3\varepsilon} = 0.2$, respectively,
t	–	time.

The k-ε model could be only used for modeling turbulence in a distance from the wall. Therefore, in case of honeycomb seal functions describing the flow near the wall averages the results.

3 Seal geometry

The geometry of the seal assumed in the calculations is presented in Fig. 2. The calculations were performed for following parameters [3]:

amount of sealing chambers, n:	10,
length of the seal, L:	0.05 m,
depth of the sealing chambers, h:	0.005 m,
diameter of the chamber, d:	0.005 m,
nominal clearance of the seal, δ:	0.0005 m,
radius of curvature, R:	0.35 m.

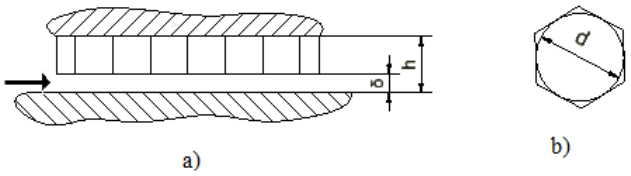

Figure 2. Dimensions of the honeycomb seal assumed in the calculations: a) side view on the seal, b) view on the single seal chamber.

The calculations were performed for three different geometries, one two-dimensional case and two three-dimensional. Every geometry was created in Gambit program. The 2D case was created from the plane that cut through the seal parallel to the flow direction. The geometry obtained in that way was basically a representation of labyrinth seal (Fig. 3). As a next step the 3D geometries were created, main task in this paper was to check the influence of the geometry simplification on the results, so one of the geometries was a case without the radius of curvature. This case is unrealistic if compared to real turbines, nonetheless on the given radius differences were hardly noticeable. The last geometry was almost the same as the previous 3D case, except that this time the radius of curvature was added. The example of three-dimensional geometry can be seen in Fig. 4. The case with radius of curvature was not shown due to lack of visible differences between this two models.

A grid for all three geometries were designed in the same program in which models were created. The grids consisted of 100 000, 1 164 000, and 1 000 000 cells respectively for 2D, 3D, and 3D with the radius of curvature. The grid was refined near the walls for better recreation of boundary layer.

4 Calculations

Boundary conditions were adopted to the calculations in the following manner: inlet pressure and temperature were constant and equal respectively 15 MPa and

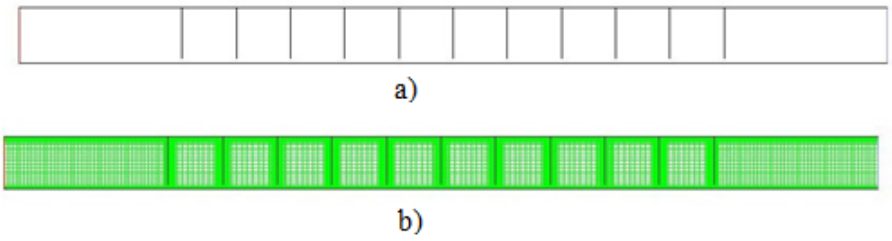

Figure 3. Geometry used in 2D calculations: a) view on the whole domain, b) grid used for the simulations.

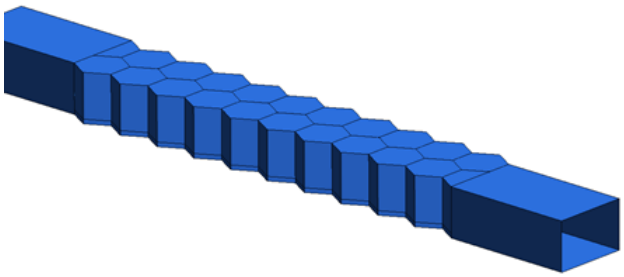

Figure 4. Geometry used for the 3D simulations.

541 °C; the outlet pressure was changed several times in order to create the flow characteristics. The different pressure values set as the outlet boundary conditions were gathered in Tab. 1. There were in total fifteen values of pressure difference per each case. Additionally the influence of the rotor movement was checked in a 3D simulations. It was achieved by setting wall movement as a boundary conditions. On a radius of 350 mm and rotation equal to 3000 rpm the linear velocity was roughly equal to 110 m/s. All this combined resulted in 75 calculation points.

Table 1. Pressure differences used in the calculations as a boundary condition.

No.	1	2	3	4	5	6	7	8	9	10	11	12	13	14	15
Δp, kPa	5	10	20	50	100	150	200	250	300	500	700	1000	1500	2000	3000

The gathered results of simulations were presented in Fig. 5. The units on the vertical axis are kg/sm, which mean that in case to obtain realistic loss numbers it just require to multiply by the circumference of the seal on certain radius. The collected data seen in Fig. 6 are surprisingly close to each other. That is why for better comparison another plot was created, in this case all results were compared

to the referenced one. Without any experiment there was a need to choose a reference case as one of the calculations result. Therefore the most complex model was chosen that is 3D case with radius of curvature and movement of rotor. Effect of this comparison was presented in Fig. 6. Surprisingly there is almost no difference between both 3D cases after reaching realistic pressure differences. With much more complex geometry the case with radius curvature shows none benefits in the obtained results. Even two-dimensional geometry after passing pressure difference of 750 kPa achieves an error that is less than 10%.

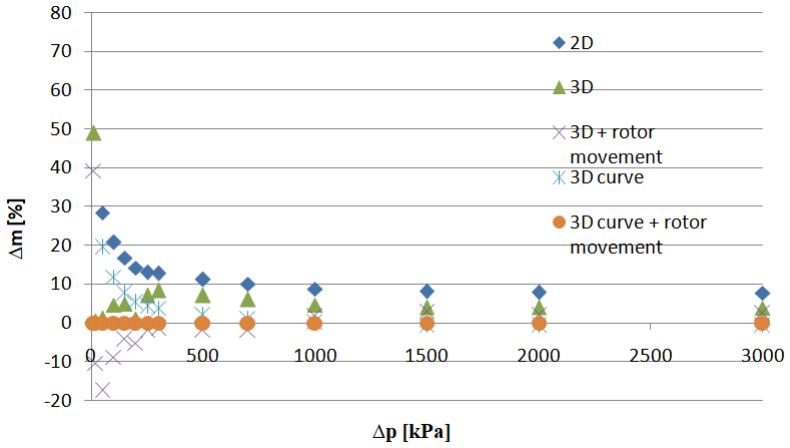

Figure 5. Percentage difference in mass flow through seal compared to the reference model.

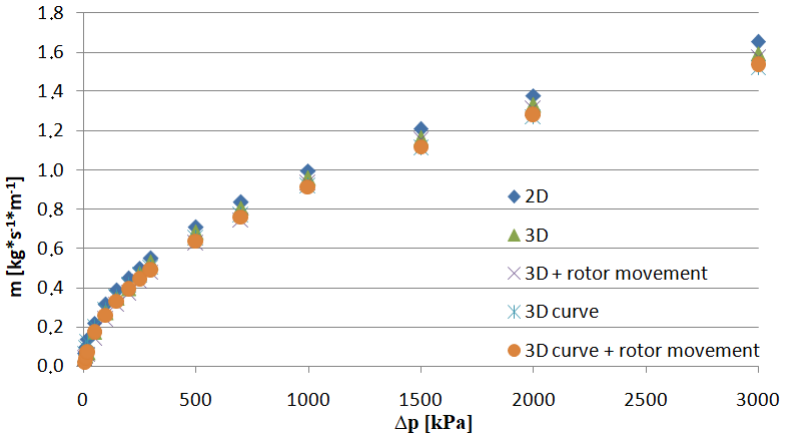

Figure 6. The flow characteristics comparison for all calculated cases.

The graphic representation of the gathered data is presented in Figs. 7 and 8. The distribution of the velocity vectors in 2D case is as in labyrinth seal but the 3D geometry gave much more interesting outcome [5,8,11]. The results presented in Fig. 9 show that in 3D model vortexes in seal chambers were much more complex and irregular. Particles whose paths are tracked, are trapped inside the seal it's because of specific geometry of honeycomb. What is interesting that the highest velocity near the very front of a seal resulted in much more rapid and intense vortexes in the first chambers of the seal.

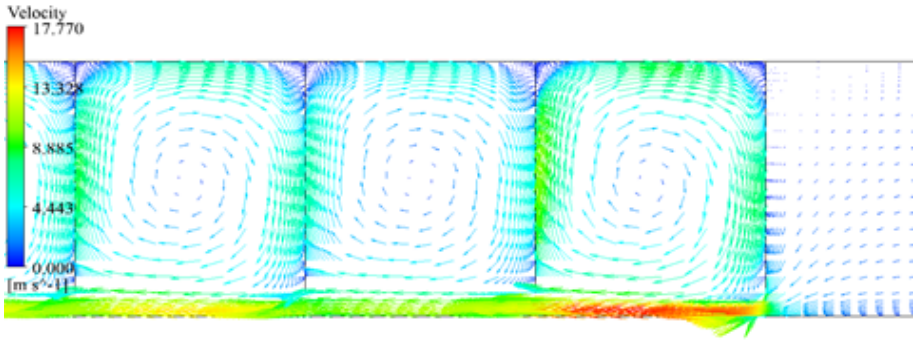

Figure 7. Velocity vectors distribution in the seal chambers.

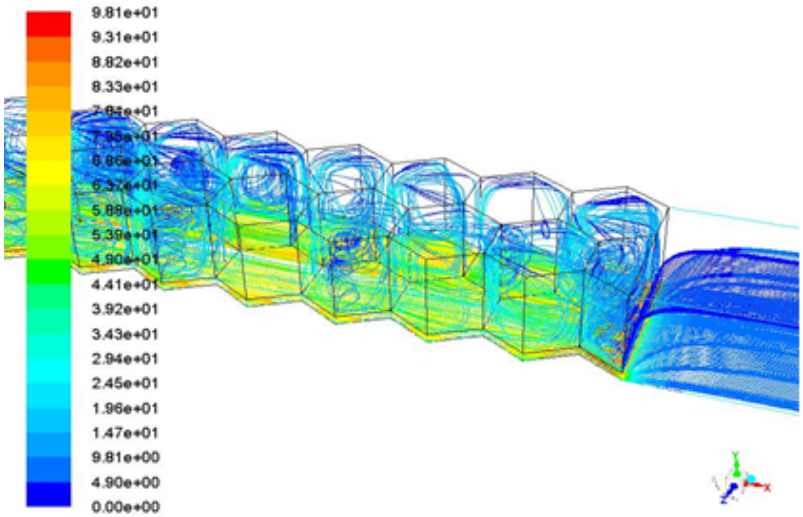

Figure 8. Pathlines of the particles traveling through the seal coloured in function of velocity.

5 Conclusions

The differences in results between both 3D cases are hardly noticeable. Therefore more complex model with radius curvature is not necessary to improve quality and accuracy of the numerical simulations. Preparing the mesh for the geometry with fillet takes much more time than the flat case and without differences which can be impactful in the designing process there is no need in performing them. Another crucial outcome is that adding rotor movement does not have as big influence as expected. The only noticeable difference is in changing of velocity vector field inside of seal chambers. Because of that vortexes are more chaotic but not to the degree where they have visible influence on the outcome of simulation. The results of 2D simulations shows that the deviation from the referenced results is almost constant after crossing point of certain operating conditions.

The CFD proved to be useful in designing and optimizing fluid flow machinery. In the literature, there are described many situations that can be solved only by the means of computer simulations. Further development on that field will result in much more efficient methods of designing process as well as diagnostics.

Received in March 2017

References

[1] Badur J.: *Five Lecture of Contemporary Fluid Termomechanics*. Gdańsk, 2005 (in Polish), www.imp.gda.pl/fileadmin/doc/o2/z3/.../ 2005_piecwykladow.pdf

[2] Bugliaev V.T., Klimtsov A.A., Perevezentsev V.T., Perevezentsev S.V.: *Honeycomb Seals in Turbomachinery*. BSTU Publisher, Bryansk 2002 (in Russian).

[3] Childs D., Elrod D., Hale K.: *Annular honeycomb seals: tests results for leakage and rotordynamic coefficients; comparison to labyrinth and smooth configurations*. J. Tribol. - T. ASME **111**(1989)2, 293–300.

[4] Chochua G., Shyy W., Moore J.: *Thermophysical modeling for honeycomb-stator gas annular seal*. In: Proc. 35th AIAA Thermophysics Conf., Anaheim, June 11–14, 2001.

[5] Choi Dong-Chun, David L., Rhode D. L.: *Development of a two-dimensional computational fluid dynamics approach for computing three-dimensional honeycomb labyrinth leakage*. J. Eng. Gas Turb. Power - T. ASME **126**(2004), 4, 794–802.

[6] Dawson M.P., Childs D.: *Measurements versus predictions for the dynamic impedance of annular gas seals-part II: smooth and honeycomb geometries*. J. Eng. Gas Turb. Power - T. ASME **124**(2002), 4, 963–970.

[7] Denton J.D.: *Loss mechanisms in turbomachines*. J. Turbomach. - T. ASME **115**(1993).

[8] Frączek D., Wróblewski W.: *Validation of numerical models for flow simulation in labyrinth seals*. J. Phys. Conf. Ser. **760**(2016).

[9] Gryboś R.: *Rudiments of Fluid Mechanics*.PWN, Warszawa 1998. (in Polish)

[10] Ha T., Childs D., Morrison G.: *Friction – factor characteristics for narrow channels with honeycomb surfaces*. J. Tribol. - T. ASME**114**(1992), 4, 714–721.

[11] Kaszowski P., Dzida M.: *CFD analysis of fluid flow through the labyrinth seal.* Trans. Inst. Fluid-Flow Mach. **130**(2015), 71–82.

[12] Kosowski K., Piwowarski M., Stępień R., Włodarski W.: *Aerodynamic forces in turbine stages.* Foundation for the Promotion of the Shipbuilding Industry and Maritime Economy, Gdańsk 2009 (in Polish).

[13] Kosowski K.: *Steam and Gas Turbines, with Examples of ALSTOM Technology.* ALSTOM Power, Elbląg 2007.

[14] Nastałek L, Karcz M., Sławiński D., Zakrzewski W., Ziółkowski P., Szyrejko C., Topolski J., Werner R., Badur J.: *On the internal efficiency of a turbine stage: classical and computational fluid dynamics definitions.* Trans. Inst. Fluid-Flow Mach. **124**(2012), 17–39.

[15] Piwowarski M., Kosowski K.: *Seals of steam turbines.* Foundation for the Promotion of the Shipbuilding Industry and Maritime Economy, Gdańsk 2009 (in Polish).

[16] D'Souza R., Childs D.: *A comparison of rotordynamic-coefficent predictions for annular honeycomb gas seals using three different friction-factor models.* Tribol. - T. ASME **124**(2002), 3, 524–529.

[17] Szymanski A., Dykas S., Wróblewski W., Majkut M., Strozik M.: *Experimental and numerical study on the performance of the smooth-land labyrinth seal.* J. Phys.: Conf. Ser. **760**(2016).

[18] Tesch K.: *Fluid Mechanics*, Gdansk University of Technology Publishing, Gdansk 2008 (in Polish) .

[19] Wasilczuk F., Flaszyńki P., Doerffer P.: *Numerical investigations of flow structure in gas turbine shroud gap.* J. Phys. Conf. Ser. **760**(2016).

[20] Ziółkowski P., Kowalczyk T., Hernet J., Kornet S.: *The thermodynamic analysis of the Szewalski hierarchic vapour cycle cooperating with a system of waste heat recovery.* Trans. Inst. Fluid-Flow Mach. **129**(2015), 51–75.